 doi:10.20944/preprints202210.0038.v1

Article

Minimalised Three-Dimensional Human Midbrain In Vitro Model for Neurotoxicity Evaluation of DYRK1 Inhibitors

Xiao Wan [1], Vincent Fagan[1,3], Paul Brennan[1,3,4], Daniel Ebner [1,*]

[1] Target Discovery Institute, Nuffield Department of Medicine, University of Oxford, Oxford, OX3 7FA, United Kingdom; xiao.pharma@gmail.com
[2] Nuleic Acid Therapy Accelerator, Research Complex at Harwell (RCaH), Rutherford Appleton Laboratory, Harwell, Didcot, Oxon OX11 0FA; xiao.wan@natahub.org
[3] Structural Genomics Consortium (SGC) University of Oxford, Oxford, United Kingdom; vinnie.fagan@gmail.com
[4] Alzheimer's Research UK, Oxford Drug Discovery Institute, Nuffield Department of Medicine, University of Oxford, Oxford, United Kingdom; paul.brennan@cmd.ox.ac.uk

* Correspondence: daniel.ebner@ndm.ox.ac.uk

Abstract: The poor success rate of preclinical drugs which target the nervous system is related to the highly complex nature of brain physiology and pathophysiology. For in vitro drug screening in this field, the two-dimensional (2D) approach - where cells are incubated in a monolayer - is not physiologically relevant. In contrast, in vivo rodent models are very low throughput and expensive. As such, improved, well-characterised three dimensional (3D) in vitro models should be employed to bridge the gap between 2D in vitro primary screening and rodent models by incorporating aspects of the in vivo brain environment. These key features include the extracellular matrix (ECM) and a multidimensional relationship of supporting cells. In this study, a neural progenitor cell line was differentiated into the main types of cells found in brain, including neurons and astrocytes. This model was designed in a 3D extracellular matrix replacement in a minimalised manner. Different culture formats using multi-well plates were explored and a high-throughput cellular imaging platform was applied. Next, we applied this model to assess neural toxicity of a newly synthesised dual-specificity tyrosine-regulated kinase 1 (DYRK1) inhibitor derived from natural compounds, which is structurally related to a natural DYRK1A inhibitor harmine, K04179. Chemical studies have already shown that K04179 has higher specificity to DYRK1A compared with previously reported DYRK1 inhibitors, such as INDY. We have produced the first report of the biological effects of this new compound on the new 3D minimalised mid-brain model with quantification of both neuronal and astrocyte populations in tandem, revealing differential toxic effects of DYRK1 inhibitor compounds K04179 and INDY on neurons and glia.

Keywords: three-dimensional in vitro model; DYRK1; human midbrain; neural progenitor cells

1. Introduction

Neural progenitor cells (NPCs) have been used as an in vitro model to study basic brain biology, functioning and physiology and have served as a platform to model human neural dysfunction for screening and the evaluation of potential treatments [1]. There is also hope that NPCs can be used as a potential strategy in regenerative medicine and treatment for traumatic brain injury [2]. Additionally, the midbrain (mesencephalon) is a region of the developing vertebrate brain that is composed of the tectum and tegmentum and this area can be particularly vulnerable to neurotoxicity [3, 4], therefore it is important to understand the unique characteristics that lead to the apparent sensitivity of this region. Unfortunately, human neural tissue is difficult to obtain, and in most cases, rodent derived cells are used as a surrogate tissue type [4, 5]. However,

Preprints (www.preprints.org) | NOT PEER-REVIEWED | Posted: 5 October 2022 doi:10.20944/preprints202210.0038.v1

rodent brain neural tissue and neural progenitor cells do not fully recapitulate human neural progenitor cell biology [6] and fail to demonstrate important pathological features - such as neurotoxicity - that are observed routinely in clinical samples [3]. In an effort to address the availability of human neural progenitor cells in biomedical research, overexpression of the myc family transcription factors in primary cells from developing mesencephalon allows the maintenance of pluripotency in two-dimensional (2D) monolayer culture [7]. This is a crucial step forward, yet the 2D method clearly lacks several very important aspects of nervous system biology, probably most importantly the three-dimensional (3D) structure of the extracellular matrix (ECM) in the brain [5].

The advantages of a 3D midbrain model will be particularly beneficial when studying the physiology and pathology related to the brain microenvironment, including the extracellular matrix and glioma, which surround the neuron network. This can be problematic when using conventional 2D monolayered assays [8] due to the difficulty in modelling 3D microenvironments in this format. Nevertheless, to date most biomedical researchers have utilised reductionist 2D models without considering that the 3D extracellular matrix (ECM) within the midbrain contains a complex 3D architecture of heterogeneous cell populations. These include neurons involved in emotion, motivation and cognition [9], as well as glial cells which provide most of the complex supporting and regulatory environment of human organs [10]. Only very recently the development of biomaterials and improvements in microfabrication have facilitated the development of in vitro models of the midbrain 3D microenvironment [5, 10, 11] which can then support the growth of glial cells (such as astrocytes) which can influence the growth of neurons in 3D in vitro models [12]. However, compared with conventional 2D models, the 3D in vitro neural models with human cells are still poorly studied, despite their potential value as research tools or therapeutics in regenerative medicine [7].

Dual-specificity tyrosine-regulated kinases (DYRKs) are members of the large CMGC kinase group. Among the DYRK family, DYRK1A is most studied due to its involvement in disorders such as Down's Syndrome [13], Parkinson's disease [14] and some cancer types [15]. DYRK1A is ubiquitously expressed in mammalian tissues with high level expression in brain development [16]. Due to the clinical significance of DYRK1A, the search for effective and selective small molecule inhibitors for DYRK1A has been of considerable interest [17], yet the complexity of this kinase has also increased interest in more fully understanding the normal biological role of DYRK1A in the brain [18]. For instance, it has been suggested that DYRK1A can regulate mouse brain and body size a dose-dependent manner [19]. Nevertheless, most of the efforts to develop novel DYRK1A inhibitors were focused on chemical potencies (Falke et al, 2015), and reports on biological effects, including toxicity, of these newly synthesised compounds are extremely limited. Therefore, applying a model which is physiologically relevant to study the neurotoxicity of DYRK1A related drug candidates is essential.

Here we describe the minimalised but physiologically relevant format of a 3D in vitro model to evaluate the effects of a novel DYRK1A inhibitor K04179, using a human mid-brain originated neural progenitor cell line ReN VM. Compared with our previous ReN VM multicellular spheroid model [28], this study integrated Matrigel as an ECM replacement, but with a minimalised volume for cost and imaging conveniency, which is described as 'sandwich culture' here. We previously reported a similar sandwich model but with cancer cells and vascular endothelial cells during a shorter culture term [16]. This is our first time investigating the long-term differentiation effects (31 days) were investigated in those neural progenitor cells cultured in Matrigel.

2. Results

Preprints (www.preprints.org) | NOT PEER-REVIEWED | Posted: 5 October 2022 doi:10.20944/preprints202210.0038.v1

2.1. Establishment of a 3D Sandwich Model of ReN cells

The workflow of 3D sandwich culture of ReN is shown in Figure 1(A). In our experience, culturing ReN on the 2D surface of conventional tissue culture treated plastic required a coating layer of extracellular matrix. With a thin coating of laminin, ReN cells grew as a monolayer, with some elongated neurite-like outgrowth suggesting neuronal differentiation after the deprivation of growth factors EGF and bFGF (Figures 1(C). The necessity of ECM coating layers suggested that ReN cells would fully reveal their capacity to differentiate into a heterogeneous group of cell subpopulations, which would better mimic the in vivo midbrain 3D structure if given a more complex and relevant substrate on which to grow.

As shown in Figure 1(C), the ReN cells cultured in 3D Matrigel sandwich developed outgrowth (indicated by arrows) after 3 days of differentiation. In addition, compared with Day 3, the areas of these 3D structures are significantly larger at Day 7. Cell seeding density was important to maintain this 3D growth manner and we found that ReN cells seeded at 1000 cells/well in a well of 96-well plate demonstrated the best maintenance of growth, as most 3D cell aggregates were formed at day 7. (See Figure s1). To evaluate if this model has the cell subpopulations more consistent of in vivo brain tissue, including neural stem cells, neurons and astrocytes, and is therefore a better model for neurotoxicity testing, we stained wells with pluripotency marker SOX2, astrocytes GFAP and neurons marker TUJ1 after treatment with a well-known neurotoxicity compound TMZ. The results on segmented areas of cell populations (Figure s2) suggested that there is significant decrease for all these three types of cells. The neurotoxicity of the compounds was evaluated using area of neurons, which is featured by neurite growth and labelled with the fluorescence intensity above the threshold stained by neuron marker Tuj1, area of astrocytes stained by the marker GFAP, and the expression of pluripotency marker SOX2. [17, 21, 22], Based on our previous studies [16, 17, 23]. Among the three cell types, the impact on astrocyte population is significant ($p = 0.047$, decrease by 5.7-fold), while the influence on the neuron population is the least (1.72-fold reduction, no significant difference). The areas marked with pluripotency marker SOX2 also showed a 2.25 folds reduction (Figure s2).

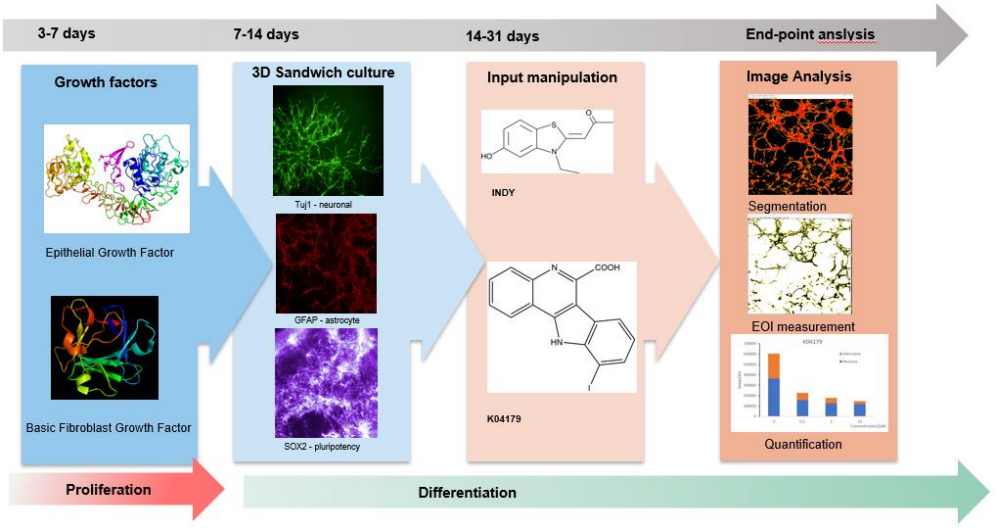

(A)

Preprints (www.preprints.org) | NOT PEER-REVIEWED | Posted: 5 October 2022 doi:10.20944/preprints202210.0038.v1

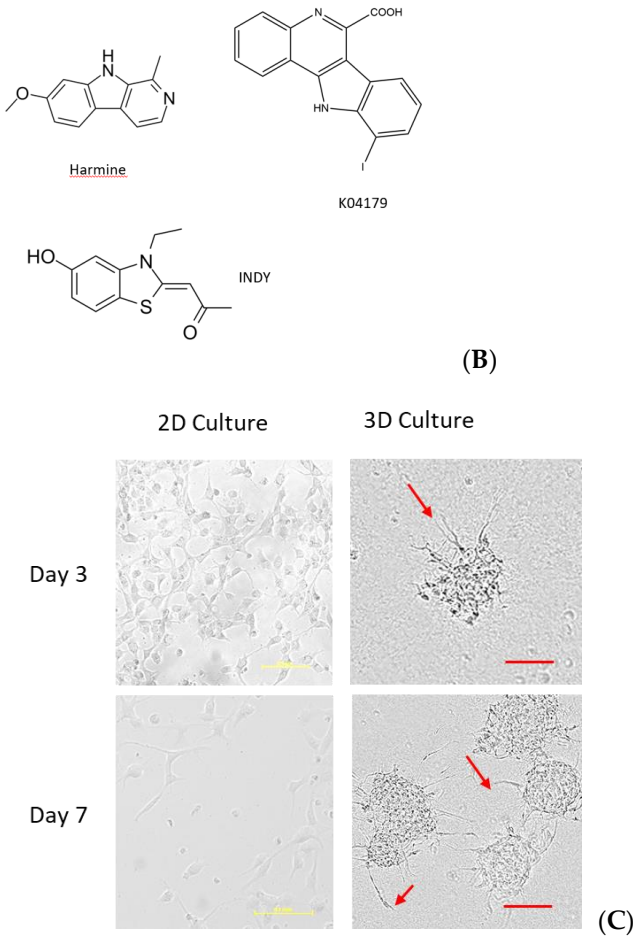

Figure 1. Workflow, chemicals and the ReN VM cell models used in the study: (A) Schematic workflows to make 3D in vitro human neural middle brain spherical and sandwich models; (**B**) Chemical structures of the compounds used in this study – K04179 is originally synthesized as an analogue to Harmine; (**C**) Morphology comparison between ReN cultured on 2D surface and ReN cultured in 3D sandwich of Matrigel and representative images of cell seeding density.

2.2. Temporal and spatial characterisation of 3D sandwich ReN model

To fully study the subpopulations derived from the ReN cells in 3D sandwich culture, we again chose three markers: SOX2 for neural stem cells, Tuj1 for neurons and GFAP for astrocytes. We explored the Z-stack imaging function of Opera Phenix and set a step of 50μm, with a total thickness of 200μm being imaged. On each layer as shown in Figure 2(A), there were both populations of astrocytes (GFAP labelled) and neurons (TUJ1 labelled). This is a good demonstration showing the 3D nature of the model, provided the minimalised sandwich format. It is also noticeable in Figure 2(A) that the contrast of signal to noise seems to remain the same throughout the thickness of all the stacks, indicating the minimalised format of the sandwich model is advantageous over more traditional 3D models such as multi-cellular spheroids which with the central areas difficult to be imaged directly. The ratios of astrocyte to neurons had some shift, which might be caused by different hypoxia microenvironment. This can be potentially improved by adding oxygen tension into the design of future models. For the quantifications of the astrocytes and neurons in Z-stack imaging please refer to Figure S3. Figure 2(B) and 2(C) suggest that at day 14 the immunofluorescence staining shows that most of the cell population expressed the astrocyte marker GFAP (red fluorescence), while at day 31 a significant number of cells expressed neuronal marker Tuj1 (green fluorescence), which altered the ratio of neurons: astrocytes from 1.54:1 (day 14) to 2.31:1 (day

Preprints (www.preprints.org) | NOT PEER-REVIEWED | Posted: 5 October 2022 doi:10.20944/preprints202210.0038.v1

31). This is consistent with previous report by other researchers that the normal ratios of neurons to astrocytes to be 2:1 to 3:1 in in vivo human brain tissue [30].

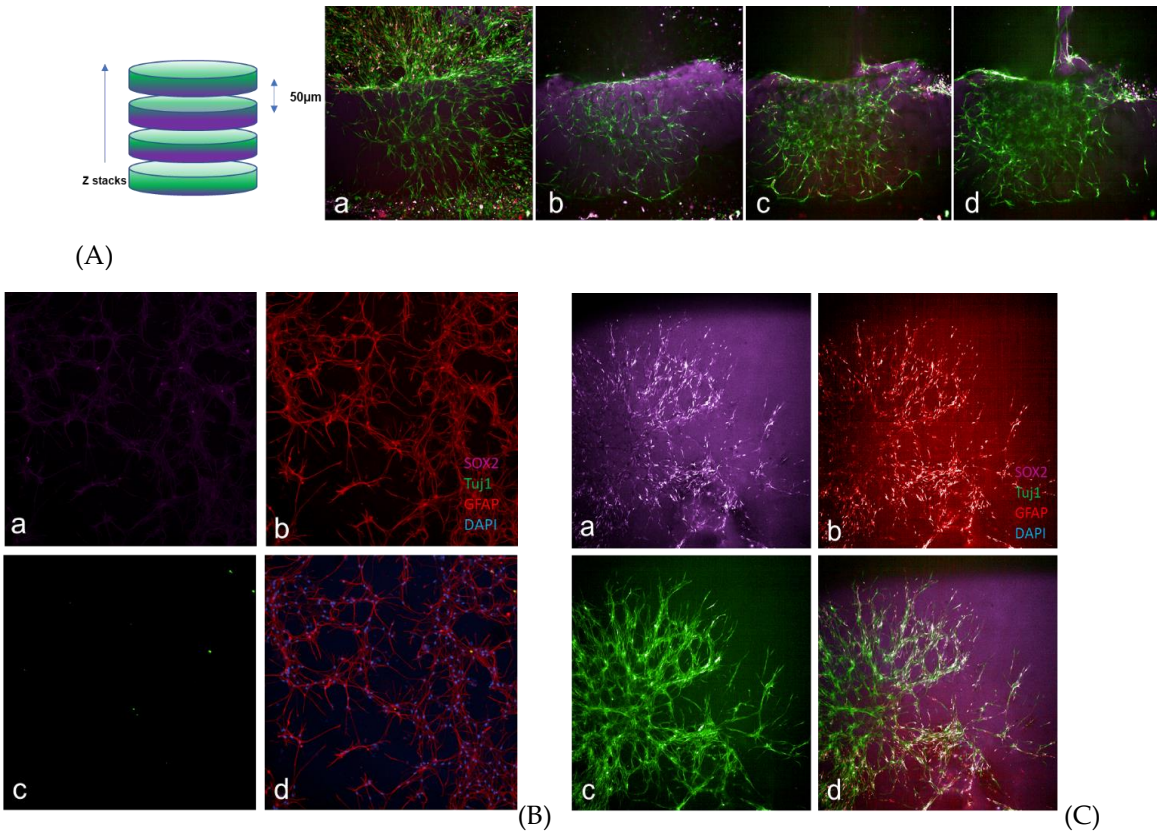

Figure 2. Spatial and temporal characterisation with multiplex immunofluorescence staining of 3D ReN sandwich model: (A) 3D z-stack imaging revealed a thickness of 200µm of the model: (a) 50µm thick; (b) 100µm thick; (c) 150µm thick; (d) 200µm thick; (B) Day 14 imaging of ReN sandwich model. The Tuj1 staining is very low; (C) Day 31 imaging of ReN sandwich model. Tuj1 is expressed by a significant population of the cells differentiated from ReN in sandwich culture.

2.3. Application of 3D sandwich ReN model for 14-day effects of DYRK1 inhibitors on neural progenitor cell differentiation

Two potent and selective inhibitors of DYRK1A were employed to evaluate the effects of DYRK1 inhibitors on neural progenitor cell differentiation: INDY [24] and the selective inhibitor K04179 (10-Iodo-11H-indolo[3,2-c]quinoline-6-carboxylic acid) [12]. The structures were shown previously in Figure 1(B). Treatment of the 3D sandwich model of ReN VM by a known DYRK1A inhibitor INDY and K04179 both suggested a potential influence on the differentiation of the ReN cells measured by segmented areas of neural marker Tuj1 and astrocyte marker GFAP. Both segmented areas and ratios of neurons to astrocytes were evaluated. Based on the areas of neurons, the DYRK1A inhibitor K04179 had a more obvious effect on the areas of neurons ($p = 0.020$) and astrocytes ($p = 0.015$), with the significant reduction of both neurons and astrocytes at a concentration as low as 0.1uM, whereas for INDY this inhibitory effect appeared at 1µM. Both INDY and K04179 had a more significant effect on reducing the astrocytes than the neurons, based on the change of the ratio between those two.

Preprints (www.preprints.org) | NOT PEER-REVIEWED | Posted: 5 October 2022 doi:10.20944/preprints202210.0038.v1

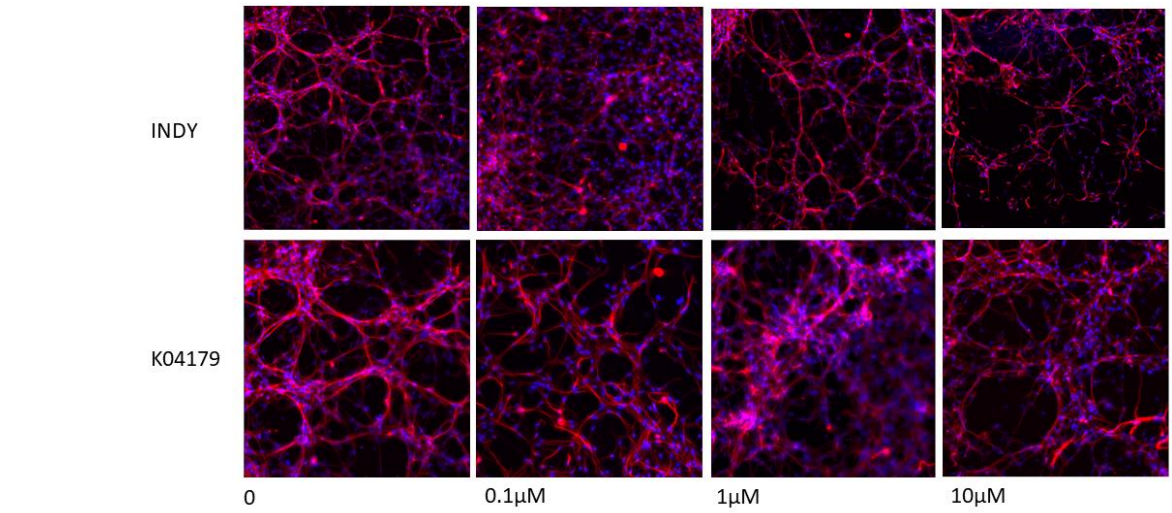

(A)

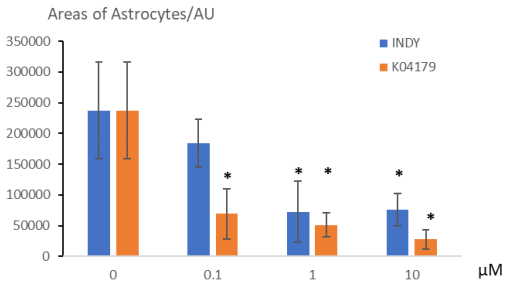

(B)

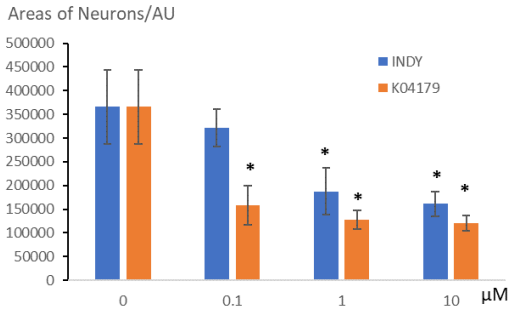

(C)

Figure 3. 14 days testing applying ReN 3D sandwich model: (A) 3D z-stack imaging revealed a thickness of 200μm of the model: (a) 50μm thick; (b) 100μm thick; (c) 150μm thick; (d) 200μm thick; (B) Day 14 imaging of ReN sandwich model. The Tuj1 staining is very low; (C) Day 31 imaging of ReN sandwich model. Tuj1 is expressed by a significant population of the cells differentiated from ReN in sandwich culture.

2.4. Application of 3D sandwich ReN model for long-term effects of DYRK1A inhibitors on neural differentiation

ReN cells were maintained in a differentiation medium for up to 31 days, and the morphology of representative samples are shown in Figure 4(A). The fluorescence labelling and analysis showed that DYRK1A inhibition by INDY decreased the areas of both neurons and astrocytes, as shown in Figure 4(B). Compared with the control group treated with DMSO only, the neuron average area of INDY treated group decreased by approximately half (68181 to 33132 AU). The group treated by K04179 is even more striking, in which the neuron area dropped to only 9505 AU compared with the DMSO treated control group (Figure s5). Interestingly, the results in Figure s4 showed some similarity, with the astrocytes were affected more significantly, with three times the difference between the control and INDY treated group (46326 AU to 14297 AU). It was noted that the cell population stained positive with the pluripotency marker SOX2 only constitutes a small faction, as we can predict that most cells differentiating into neurons or astrocytes.

Preprints (www.preprints.org) | NOT PEER-REVIEWED | Posted: 5 October 2022 doi:10.20944/preprints202210.0038.v1

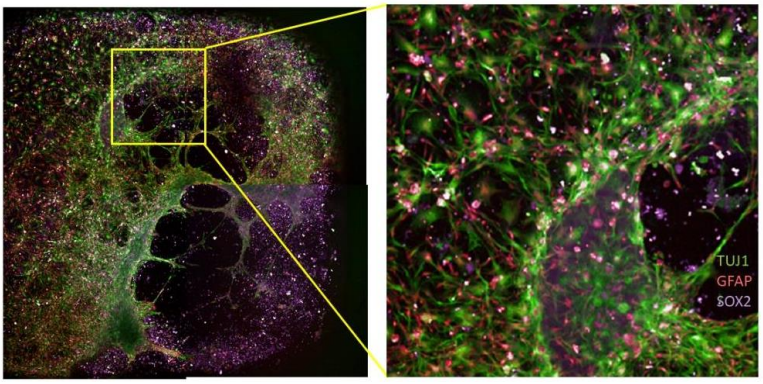

(A)

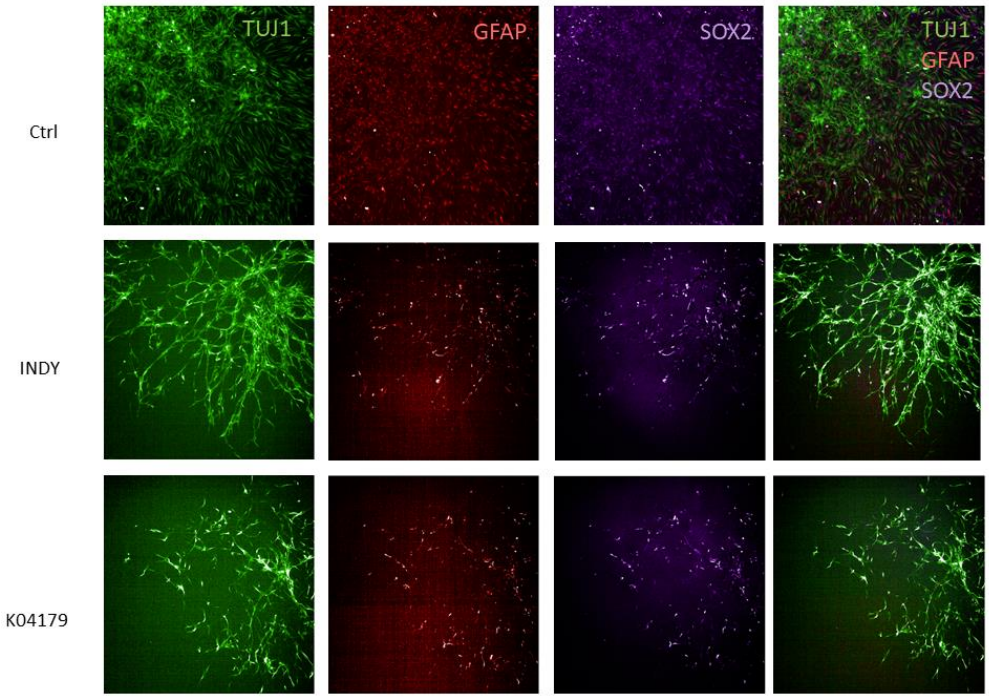

(B)

Figure 4. 31 days of long-term evaluation applying ReN 3D sandwich model: (A) A specially zoomed in figure showing the 3D microarchitecture formed by subpopulations derived from ReN cells cultured in 3D Matrigel sandwich. (B) Representative images of the dose-dependent imaging of the ReN sandwich model treated by a known DYRK1A inhibitor INDY and the new DYRK1A inhibitor K04179.

3. Discussion

Modelling human brain tissue has historically been a challenge for the scientific research community and this can be attributed to many factors, including the complexity of brain architecture, the need to co-culture several specialized cell types and the dynamics of the brain microenvironment - including, but not limited to - the ECM [5]. Therefore, by reconstituting the 3D in vitro microenvironment for neural stem cells, these cells can adopt a more physiologically relevant and robust phenotype suitable for screening purposes [10], Shin, Yang [19], [27, 28]. In this study, we chose the commercially available neural progenitor cell line ReN from the midbrain (ReN VM) to establish our platform, given their immortality, ability to be readily differentiated into neurons and glial cells and their rapid growth on laminin in the expansion stage [11]. Our approach utilises minimalised sandwich format, where the cells exhibit distinct morphological features that are more physiologically representative than 2D culture. There has been some attempts to employ ReN cells to model the neural degradation process

 doi:10.20944/preprints202210.0038.v1

previously [11]; however, these protocols took several months to complete and were carried out in a low throughput format. Importantly, here we have generated a method that is both more time efficient and conducive to high throughput screening, including a multiplexed analysis paradigm: 1. The through-put has been increased to 384-well plate format; 2. A more multiplexed analysis paradigm was applied, including neural marker Tuj1, astrocyte marker GFAP and pluripotency marker SOX2; 3. A recently reported DYRK1A inhibitor K04179 was synthesised and tested, together with a range of reported DYRK1A inhibitors such as INDY. This is the first biological study on this relatively novel compound; 4 Because a Matrigel sandwich was applied to create 3D environment rather than a Matrigel embedding protocol, technically this will allow the automatic processing of the washing and staining procedures. We also tested the front-line chemotherapy reagent temozolomide (TMZ), an alkylating agent used as a treatment of some brain cancers, considered as a model compound to evaluate the potential of our 3D culture in the application of neurotoxicity testing (Figure s2). It has been reported that DYRK1A could be a potential target for glioblastoma [25], and the neurotoxicity caused by this first-line chemotherapy drug has been investigated [26], so it would be valuable to demonstrate if our ReN sandwich model respond to the treatment of this compound through cellular morphology.

In this study, we chose the commercially available neural progenitor cell line ReN from the midbrain (ReN VM), considering its advantages such as immortality, abilities to be readily differentiated into neurons and glial cells, rapid growth on laminin layer in expansion stage [11]. Both short-term (14 days) and relatively long-term culturing end-points (31 days) were investigated. The neuron: astrocyte ratio increased from day 7 to day 31 among the ReN cell populations in 3D sandwich culture; this mimics the natural differentiation process of neural progenitor cells, in which glial marker are expressed followed by neuronal markers [29]. Observations carried out regarding both acute neurotoxicity and intervention using small compounds on long-term neural development demonstrated the potential of DYRK1A to influence this important phenotype feature. The neurotoxicity of the compounds was measured by a few parameters, the first being the area of neurons, which are labelled with the fluorescence intensity above the threshold stained by neuron marker Tuj1, which also demonstrated a morphology of neurite growth. The area of astrocytes was also quantified, by segmentation using staining by the marker GFAP. In addition, expression of pluripotency marker SOX2 was also considered. The choice of these parameters are adapted from previous reports [21] [22] [17]. In addition, we discovered that after 14 days of differentiation, the ReN cells could be differentiated into a significant population of astrocytes (the ratio of neuron to astrocyte was 1.54:1). After 31 days of differentiation, neuron marker Tuj1 was expressed by a greater number of cells (the ratio of neuron to astrocyte increased to 2.31:1). Based on previous studies, researchers reported the normal ratios of neurons to astrocytes in human brain to be 2:1 to 3:1 [30]. Thus a key experimental feature of our model is that the ratio falls into this physiological range after 31 days of culture and differentiation.

The DYRK1 family of proteins has been considered as a target for intervention of neural development and degradation pathologies. Reports have demonstrated the potential of targeting DYRK1A using rodent-based midbrain derived cells [15, 24]. However, considering the difference between rodents and humans, our physiologically relevant human cell-derived model to study this attractive target is important for the field. We demonstrated the feasibility of applying our ReN 3D model to investigate the neurotoxicity of DYRK1A inhibitors, by quantifying the neuron and astrocyte cell populations. We discovered that the more specific DYRK1A inhibitor K04179 had a more obvious effect compared with INDY regards to decreasing the area of neurons and astrocytes. Both INDY and K04179 had a more significant effect on reducing the astrocytes numbers than the neurons, based on the change of the ratio between the two. This demonstrates that even when targeting the same kinase, different inhibitors can have different toxicity

Preprints (www.preprints.org) | NOT PEER-REVIEWED | Posted: 5 October 2022 doi:10.20944/preprints202210.0038.v1

profiles. In this case, INDY is a potent and ATP-competitive Dyrk1A and Dyrk1B inhibitor with IC50s of 0.24 μM and 0.23 μM, respectively [12], while the IC50 of K04179 for DYRK1A is as low as 6nM, and IC50 for DYRK1B is 600nM, as previously reported (Falke et al, 2015). Novel inhibitors presumably with higher specificity still needs particular careful investigation regarding both efficiency and toxicity. A recent report has shown the influence of DRK1A inhibition on vascular dysfunction in the context of developing cerebral vasculature via regulation of calcium signalling, using a zebrafish model [31]. In our previous report, a similar 3D sandwich model demonstrated its potential application in angiogenesis study [16]. We propose that the ReN sandwich 3D model in this study, once integrated with human endothelial cells, can also be employed to further confirm the discoveries found using other animal models with significant 3Rs (replacement, reduction and refinement for animals in research) impact.

We also explored the possibility of scaling-up this 3D model with a high-throughput imaging system and 384-well plate format. Future studies using this model can expand the profiling to include other phenotypic measurements; for example, the production of reactive oxygen species, inflammatory factors [3], the reduction of dopamine levels or the absorption and storage of synaptic vesicles [4]. Another aspect to investigate further is to further define the ECM used in the 3D sandwich model. Matrigel is a hydrogel derived from mouse Englebreth-Holm-Swarm tumours, containing a mixture of laminin, collagen and other growth factors [32]. This provides a good starting point to mimic certain aspects of extracellular matrix to maintain the pluripotency of stem cells, and to restore other physiologically relevant behaviours of other cell types such as vascular endothelial cells [17]. However, the complexity of its components also require careful interpretation and its sensitivity to temperature change limits its application [32]. Although the image analysis methods described here was done manually, the workflow is scalable as the image acquisition was done on the mainstream high-throughput imaging platform Opera Phenix and stored in Columbus. The add-on of high-throughput expertise to address this is a possible capacity. There are also other steps which can be integrated into the workflow to increase the throughput, such as applying Janus automatic liquid handling system. There are limitations which need to be taken into considerations, including the evaporation of the wells at the edge – in this study, the wells at the four edges were not used for cell culture, but were filled with PBS instead. In addition, these will be topped up every three days. The suggested volumes of the added reagents for scaling-up of the model for high-throughput are listed in Table 1.

Table 1. Scale-up of 3D sandwich model of ReN human midbrain for higher throughput potential.

Steps in order	24-well plate	96-well plate	384-well plate
Max working volume (μL)	3000	200	80
Bottom layer of Matrigel(μL)	100-120	15-20	9
ReN VM cells per well	15000	1000	400
Top medium with 5% Matrigel (μL)	1000	100	60
4% FPA fixation (μL)	100-150	30-50	6-10
PBS-glycine neutralisation(μL)	300	100	20
Blocking buffer (μL)	150-200	50-100	10-20
Antibody dilution buffer (μL)	150-200	50-100	10-20
Wash buffer (IF buffer or PBS)(μL)	300-600	100-200	20-40
Mounting buffer (μL)	150-200	50-100	6-10

Combined with the benefit of greatly reducing the issues associated with in vivo rodent models, including overall numbers of animals, cost, ethics, and potential animal welfare burden, we feel that improved, well developed 3D in vitro models as described here continue to provide a crucial tool to evaluate the neurotoxicity of therapeutics and to study other pharmacological and physiological microenvironment factors.

 doi:10.20944/preprints202210.0038.v1

4. Materials and Methods

4.1. Maintenance of ReN VM cells

Tissue culture treated culture flasks or well-plates were coated with laminin diluted 1:100 in ReN maintenance medium (Merck Millipore), then the cells were thawed based on supplier's instructions (Merck Millipore) and expanded in ReN growth medium, which is the ReN maintenance medium supplemented with EGF 20ng/mL, bFGF 20ng/mL. Before the 3D culture, all the cells were cultured in a humidified incubator at 37°C with 5 % CO2. Once 70% confluency was reached, the ReN VM cells were passaged with accutase solution (Gibco).

4.2. 3D Sandwich culture and differentiation of ReN

A modified 3D culture protocol was developed to form the Matrigel sandwich structure based on our previous method [16]. Briefly, to form the bottom layer of Matrigel, 120µL pure Matrigel (Corning, 354230) was added into each well which had been pre-chilled on ice, and then the plates were incubated at 37°C for 30min, allowing the Matrigel to polymerise. Then ReN VM were seeded onto the polymerised gel layer at the density of 1.4×10^5 cells/mL, in 250µL neural growth medium, which is made of neural basal medium (Merck Millipore) supplemented with 20ng/mL EGF and 20ng/mL bFGF. After 4 hours of cell seeding, 10% Matrigel (v/v) in 250µL neural growth medium was added onto the polymerised structure. The plate was then left at 37oC to allow the top layer of Matrigel to polymerise. The ReN VM sandwich 3D model system was maintained in neural growth medium at 37°C, 5% CO_2 for at least 24 hours before further drug testing. The ReN VM cells were differentiated using a growth factor deprivation protocol based on the instruction of the supplier.

4.3.Testing of DYRK1 inhibitors and TMZ

INDY was purchased from Sigma-Aldrich, Temozolomide (TMZ) was purchased from Cambridge Bioscience (UK) and K04179 was synthesized as previously described [12]. It is noticeable that K04179 was originally discovered to have high affinity to DYRK1A as an analogue to known DYRK1A inhibitor Harmine, as shown in Figure 1(B). The stock solutions were prepared at the concentration of 10mM in DMSO and stored at -80°C for up to six months. When used, the stock solution was diluted by ReN maintenance medium to the desired concentrations.

The tested compounds were added in the neural basal medium for designed end-point assays for 14 days and 31 days. The compounds were applied at concentrations ranging from 0.1, 1, to 10µM. The compounds were added to the 3D in vitro models 24 hours after the cell seeding and gel polymerisation, based on previous studies [16, 17, 20]. The whole workflow of differentiation and treatment with compounds followed by image analysis is shown in Figure 2(A). The culture was maintained and analysed at day 14 for neurotoxicity, and day 31 for a long-term differentiation evaluation assay respectively.

4.4. 3D culture whole fixation Immunofluorescence

Cells in 3D culture were stained using a protocol modified for sandwich Matrigel [16, 17]. The samples were first fixed with 4% PFA for 30 minutes at room temperature, then neutralised and washed using PBS - glycine (100mM glycine in PBS) two times, then blocking buffer (10% goat serum (Sigma), 1% goat F(ab')2 anti-mouse immunoglobulin G (ThermoFisher, A24514) in staining buffer (PBS supplemented with 0.2% TritonX-100, 0.1% BSA, and 0.05% Tween 20) was added. The samples were then incubated with primary antibodies at 4oC overnight, followed by incubation in a suitable second

Preprints (www.preprints.org) | NOT PEER-REVIEWED | Posted: 5 October 2022 doi:10.20944/preprints202210.0038.v1

antibodies (Human anti-rat Alexa 555 A21434, human anti-rabbit Alexa 488 A27034) at room temperature for 45 minutes and finally were mounted with diaminophenylindole (DAPI) mounting medium (Abcam, UK). Images were taken and processed on a confocal microscope (Nikon, UK). Vendor details are listed in Table s1, and further information on working solution preparation is listed in Table s2.

4.5. Analysis of multiplexed immunofluorescence staining of ReN sandwich models

The images were taken on high-throughput imaging platform Opera Phenix (Perkin-Elmer), with the 10× object lens. We employed ImageJ to quantify the fluorescence images. Briefly RGB images were converted into 8-bit type, then the channels were split using 'colour – split channels' in the 'image' section. The images were then segmented using 'image-adjust-threshold' function. The intensity segmentation threshold was set as an averaged value between 36 to 64, after a pre-test of a subpopulation of 25% of the whole image population. Then the objects were treated as 'particles' and counted using 'analyse-particles' function, with a size filter set as between 20 to 100µm (a representative image segmented is shown in Figure 2B. For 14 days neurotoxicity testing, both the cell numbers and areas after segmentation were monitored. For 31 days differentiation evaluation, the neuron-astrocyte ratios were calculated as N (number of green fluorescent particles segmented)/N (number of red fluorescent particles segmented). For area measurement, the same segmentation process was applied for the group at day 14, except that an extra step was applied using the function 'Edit – selection – create selection', and the areas of interest (EOI) were then measured.

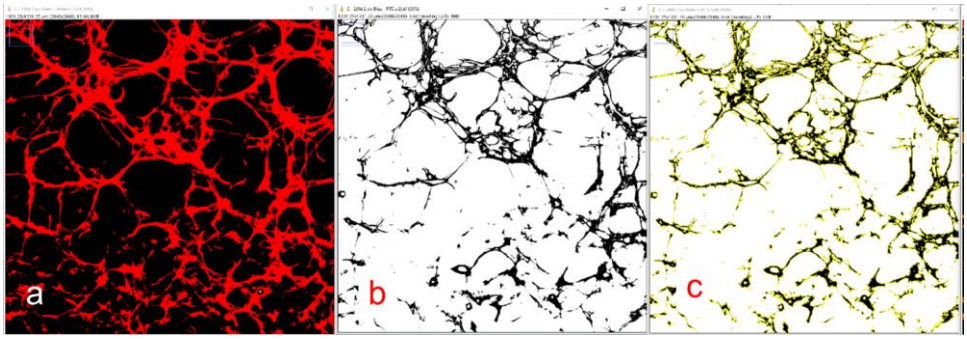

Figure 5. Multiplexed immunofluorescence imaging and processing: (a) Image processing sequence; (b) Set fluorescence intensity segmentation; (c) Set particle size filter as 20-100µm prior to counting.

Author Contributions: XW designed the project, carried out the experiments and wrote the manuscript. VF synthesized the DYRK1A inhibitor and edited the manuscript; PB provided resources to synthesize the DYRK1A inhibitor; DE provided the resources for the experiments, edited the manuscript and supervised the project.

Funding: Xiao Wan was a Training Fellow sponsored by National Centre for the Replacement, Refinement & Reduction of Animals in Research (NC3Rs, UK), grant number NC/P002374/1. Peter Oliver (Nucleic Acid Therapy Accelerator, Medical Research Council) edited the article, and kindly provided detailed advice on neurobiology. Aparna Sinha kindly provided advice on the potential of scalability of this model. Anna Malinowska (Nucleic Acid Therapy Accelerator, Medical Research Council) kindly provided the chemical structure drawing. Andres Correa-Sanchez (Nucleic Acid Therapy Accelerator, Medical Research Council) kindly provided guidance on target validation. Val Miller (Target Discovery Institute, University of Oxford) kindly provided help with image acquisition. Francesca Nicolls (Target Discovery Institute, University of Oxford) has kindly provided advice on the in vivo anatomy of the brain. Paul Brennan was supported by Alzheimer's Research UK (ARUK-2018DDI-OX).

Institutional Review Board Statement: Not applicable;

Preprints (www.preprints.org) | NOT PEER-REVIEWED | Posted: 5 October 2022 doi:10.20944/preprints202210.0038.v1

Informed Consent Statement: Not applicable

Data Availability Statement: Data will be archived in Bodleian Libraries.

Acknowledgments: Dr Francesca Nicolls (Target Discovery Institute, University of Oxford) has kindly provided advice on the in vivo anatomy of the brain. Mr Mataka Banda kindly provided some proof-reading help. Miss Aparna Sinha helped with imaged analysis. Dr Anna Malinowska helped with the chemical structure drawing. Dr Peter Oliver generously helped with the writing of the manuscript.

Conflicts of Interest: The authors declare no conflict of interest.

Appendix A – supplementary figures

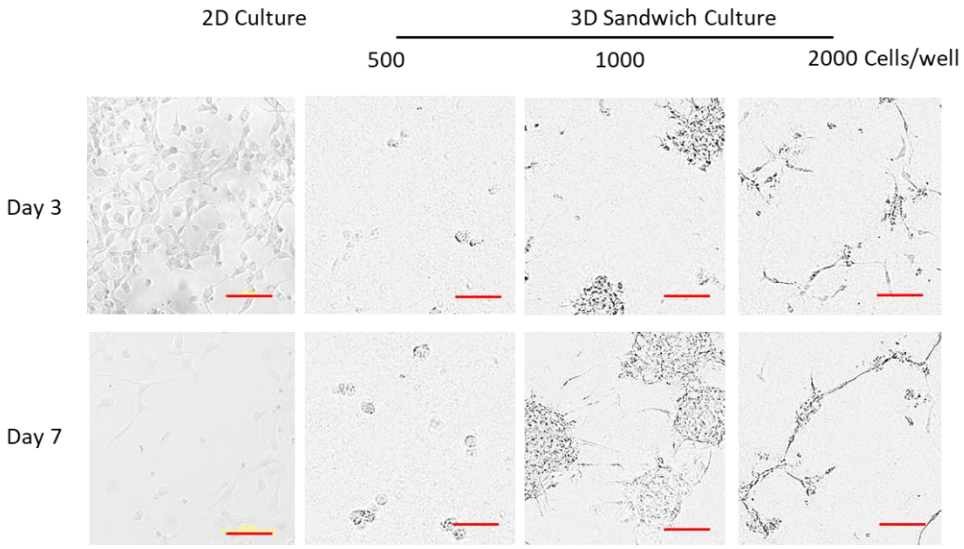

Figure S1. Cell seeding density optimization

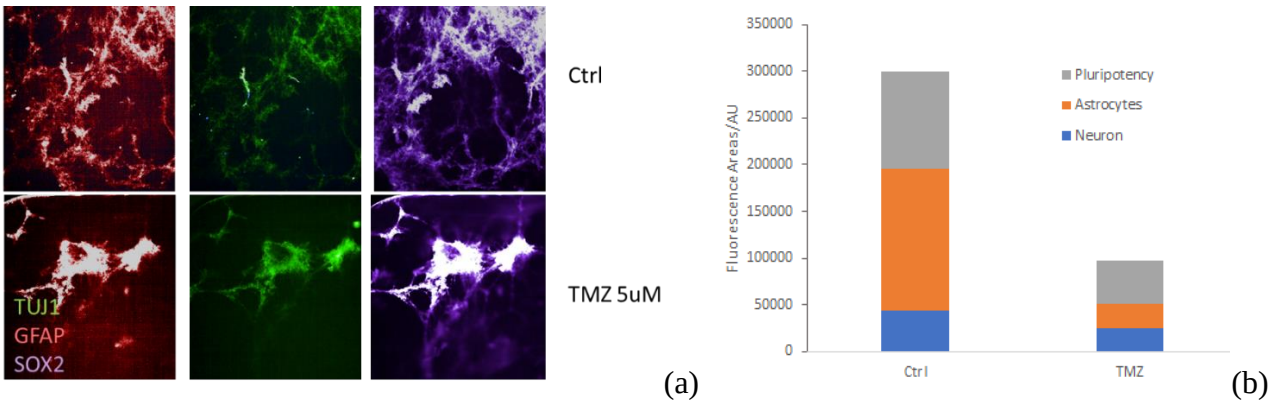

Figure S2. A widely accepted compound TMZ showed effects on cell subpopulations in the ReN 3D model established in this study (a) Representative pictures of 3D ReN sandwich culture in the absence and in the presence of temozolomide (TMZ) 5μM treatment for 5 days (b) Quantification of fluorescence areas of 3D ReN sandwich culture compared with control group.

Preprints (www.preprints.org) | NOT PEER-REVIEWED | Posted: 5 October 2022 doi:10.20944/preprints202210.0038.v1

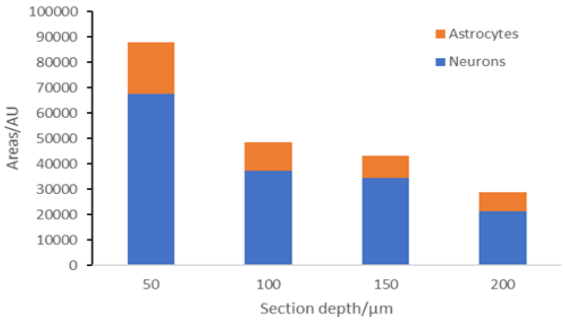

Figure S3. Quantification of astrocytes to neuron ratios based on the Z-stack scanning depths.

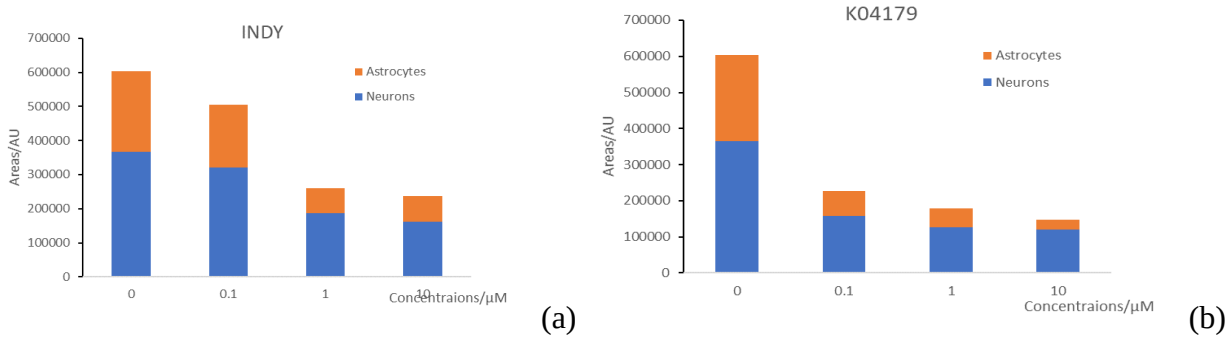

Figure S4. Ratio of astrocytes and neurons over the 14 days.

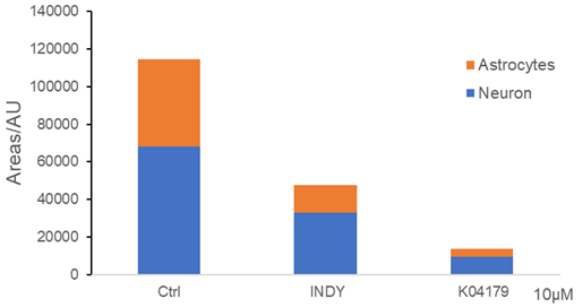

Figure S5. Quantification of the multiplexing staining of the ReN sandwich model after 31 days of treatment by 10μM of INDY and K04179.

Appendix B – Table s1. A list of the antibodies used in the study

Title 1	Cat. No.	Suppliers
Mouse anti-human SOX2	MAB4423	Merck Millipore
Rat anti-human GFAP (2.2 B10)	13-0300	Thermo-
Rabbit anti-human Tuj1	Ab18207	Abcam
Goat anti-rat Alexa 555	A21434	Thermo
Goat anti-rabbit super clonal Alexa 488	A27034	Thermo-Fisher
Goat anti-mouse Alexa 630	Ab150115	Abcam

References

1. Walker, T., J. Huang, and K. Young, Neural Stem and Progenitor Cells in Nervous System Function and Therapy. Stem cells international, 2016. 2016: p. 1890568-1890568.

2. Takahashi, J., Stem cells and regenerative medicine for neural repair. Curr Opin Biotechnol, 2018. 52: p. 102-108.
3. Kraft, A.D. and G.J. Harry, Features of microglia and neuroinflammation relevant to environmental exposure and neurotoxicity. International journal of environmental research and public health, 2011. 8(7): p. 2980-3018.
4. Ma, K., et al., Neurotoxicity effects of atrazine-induced SH-SY5Y human dopaminergic neuroblastoma cells via microglial activation. Molecular BioSystems, 2015. 11(11): p. 2915-2924.
5. Sood, D., et al., 3D extracellular matrix microenvironment in bioengineered tissue models of primary pediatric and adult brain tumors. Nature Communications, 2019. 10(1): p. 4529.
6. Wang, H., Modeling Neurological Diseases With Human Brain Organoids. Frontiers in synaptic neuroscience, 2018. 10: p. 15-15.
7. Donato, R., et al., Differential development of neuronal physiological responsiveness in two human neural stem cell lines. BMC neuroscience, 2007. 8: p. 36-36.
8. Jo, J., et al., Midbrain-like Organoids from Human Pluripotent Stem Cells Contain Functional Dopaminergic and Neuromelanin-Producing Neurons. Cell Stem Cell, 2016. 19(2): p. 248-257.
9. Jorfi, M., et al., Three-Dimensional Models of the Human Brain Development and Diseases. Advanced healthcare materials, 2018. 7(1): p. 10.1002/adhm.201700723.
10. Wan, X., E. O'Neill, and D. Ebner, 5.41 - In Vitro Cancer Models☆, in Comprehensive Biotechnology (Third Edition), M. Moo-Young, Editor. 2019, Pergamon: Oxford. p. 550-559.
11. Choi, S.H., et al., A three-dimensional human neural cell culture model of Alzheimer's disease. Nature, 2014. 515: p. 274.
12. Falke, H., et al., 10-iodo-11H-indolo[3,2-c]quinoline-6-carboxylic acids are selective inhibitors of DYRK1A. Journal of medicinal chemistry, 2015. 58(7): p. 3131-3143.
13. Wegiel, J., C.-X. Gong, and Y.-W. Hwang, The role of DYRK1A in neurodegenerative diseases. The FEBS journal, 2011. 278(2): p. 236-245.
14. Barallobre, M.J., et al., DYRK1A promotes dopaminergic neuron survival in the developing brain and in a mouse model of Parkinson's disease. Cell death & disease, 2014. 5(6): p. e1289-e1289.
15. Birger, Y. and S. Izraeli, DYRK1A in Down syndrome: an oncogene or tumor suppressor? The Journal of clinical investigation, 2012. 122(3): p. 807-810.
16. Wan, X., et al., Morphological analysis of human umbilical vein endothelial cells co-cultured with ovarian cancer cells in 3D: An oncogenic angiogenesis assay. PloS one, 2017. 12(7): p. e0180296-e0180296.
17. Wan, X., et al., Perfused Three-dimensional Organotypic Culture of Human Cancer Cells for Therapeutic Evaluation. Scientific Reports, 2017. 7(1): p. 9408.
18. Jessberger, S., Stem Cell-Mediated Regeneration of the Adult Brain. Transfusion medicine and hemotherapy : offizielles Organ der Deutschen Gesellschaft fur Transfusionsmedizin und Immunhamatologie, 2016. 43(5): p. 321-326.
19. Shin, Y., et al., Reconstituting vascular microenvironment of neural stem cell niche in three-dimensional extracellular matrix. Adv Healthc Mater, 2014. 3(9): p. 1457-64.
20. Wan, X., et al., Three-dimensional perfused tumour spheroid model for anti-cancer drug screening. Biotechnology Letters, 2016. 38: p. 1389-1395.
21. Gornstein, E.L. and T.L. Schwarz, Neurotoxic mechanisms of paclitaxel are local to the distal axon and independent of transport defects. Experimental neurology, 2017. 288: p. 153-166.
22. O'Callaghan, J.P. and K. Sriram, Glial fibrillary acidic protein and related glial proteins as biomarkers of neurotoxicity. Expert Opin Drug Saf, 2005. 4(3): p. 433-42.
23. Ahmed, A.A., et al., The extracellular matrix protein TGFBI induces microtubule stabilization and sensitizes ovarian cancers to paclitaxel. Cancer Cell, 2007. 12(6): p. 514-27.
24. Abbassi, R., et al., DYRK1A in neurodegeneration and cancer: Molecular basis and clinical implications. Pharmacology & Therapeutics, 2015. 151: p. 87-98.
25. Pozo, N., et al., Inhibition of DYRK1A destabilizes EGFR and reduces EGFR-dependent glioblastoma growth. The Journal of Clinical Investigation, 2013. 123(6): p. 2475-2487.
26. Yoshimura, J., et al., The effects of temozolomide delivered by prolonged intracerebral microinfusion against the rat brainstem GBM allograft model. Childs Nerv Syst, 2012. 28(5): p. 707-13.
27. Wan, X., W. Wang, and Z. Liang, Epigallocatechin-3-gallate inhibits the growth of three-dimensional in vitro models of neuroblastoma cell SH-SY5Y. Molecular and Cellular Biochemistry, 2021. 476(8): p. 3141-3148.
28. Wan, X., et al., ReN VM spheroids in matrix: A neural progenitor three-dimensional in vitro model reveals DYRK1A inhibitors as potential regulators of radio-sensitivity. Biochemical and Biophysical Research Communications, 2020. 531(4): p. 535-542.
29. Hong, Y.J. and J.T. Do, Neural Lineage Differentiation From Pluripotent Stem Cells to Mimic Human Brain Tissues. Frontiers in Bioengineering and Biotechnology, 2019. 7(400).
30. Herculano-Houzel, S., The Glia/Neuron Ratio: How it Varies Uniformly Across Brain Structures and Species and What that Means for Brain Physiology and Evolution. Glia, 2014. 62.
31. Cho, H.-J., et al., Vascular defects of DYRK1A knockouts are ameliorated by modulating calcium signaling in zebrafish. Disease Models & Mechanisms, 2019. 12(5): p. dmm037044.
32. Hughes, C.S., L.M. Postovit, and G.A. Lajoie, Matrigel: A complex protein mixture required for optimal growth of cell culture. PROTEOMICS, 2010. 10(9): p. 1886-1890.